Supplementary Information

Stem Cell-Derived Exosomes as Nanotherapeutics for Autoimmune and Neurodegenerative Disorders

Milad Riazifar[†,■], M. Rezaa Mohammadi[‡,■], Egest J. Pone[†,§], Ashish Yeri[‖], Cecilia Lässer[⊥], Aude I. Segaliny[†], Laura L. McIntyre[#], Ganesh Vilas Shelke[⊥,¶], Elizabeth Hutchins[‖], Ashley Hamamoto[†], Erika N. Calle[†], Rossella Crescitelli[⊥], Wenbin Liao[†], Victor Pham[†], Yanan Yin[□], Jayapriya Jayaraman[†], Jonathan R.T. Lakey[Δ], Craig M. Walsh[#], Kendall Van Keuren-Jensen[‖], Jan Lotvall[⊥], Weian Zhao[†, *]

[†]Department of Pharmaceutical Sciences, Sue and Bill Gross Stem Cell Research Center, Chao Family Comprehensive Cancer Center, Edwards Life Sciences Center for Advanced Cardiovascular Technology, Department of Biomedical Engineering, and Department of Biological Chemistry, University of California, Irvine, CA, 92697, USA.

[‡]Department of Materials Science and Engineering, University of California, Irvine, CA, 92697, USA.

[§]Department of Physiology & Biophysics, Vaccine Research & Development Center, University of California, Irvine, CA, 92697, USA.

[‖]Neurogenomics Division, Translational Genomics Research Institute, Phoenix, AZ, 85004, USA

[⊥]Krefting Research Centre, Institute of Medicine, The Sahlgrenska Academy, University of Gothenburg, Gothenburg 40530, Sweden.

[#]Department of Molecular Biology and Biochemistry, Sue and Bill Gross Stem Cell Center, Multiple Sclerosis Research Center, University of California, Irvine, Irvine, CA 92697, USA

[¶]Department of Surgery, Institute of Clinical Sciences, University of Gothenburg and Sahlgrenska University Hospital, Gothenburg, Sweden.

[□]Department of Biochemistry and Molecular Cell Biology, Shanghai Jiao Tong University School of Medicine, Shanghai 200025, China

[Δ]Department of Surgery, University of California, Irvine, Orange, CA, 92868, USA

[■]M. Riazifar and M. R. Mohammadi contributed equally to this work

* Correspondence should be addressed to W. Z. (weianz@uci.edu)

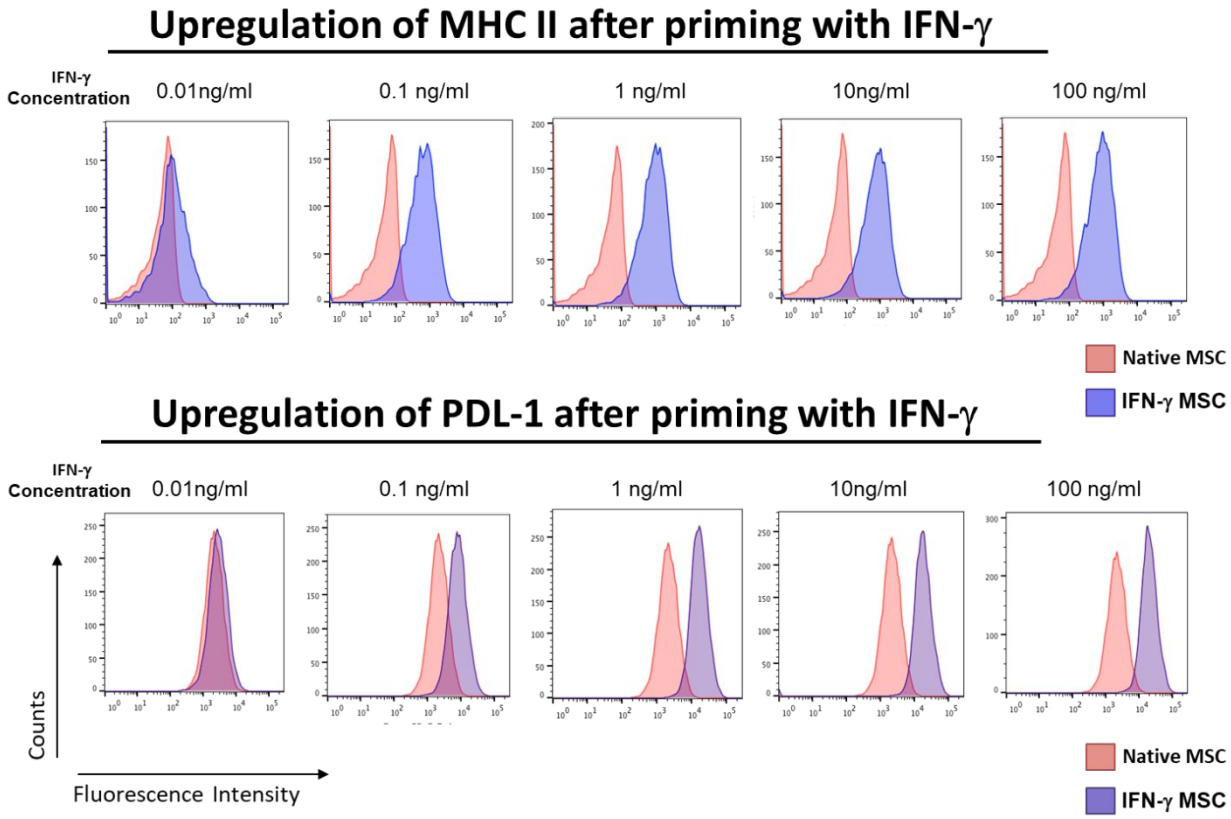

Figure S1. Flow cytometry analyses show upregulation of major histocompatibility complex II (MHCII) (Top panel) and programmed death-ligand 1 (PD-L1) (bottom panel) expression on MSCs under different concentrations of IFNγ compared to Native MSCs. 10 ng/ml IFNγ was eventually chosen for the study.

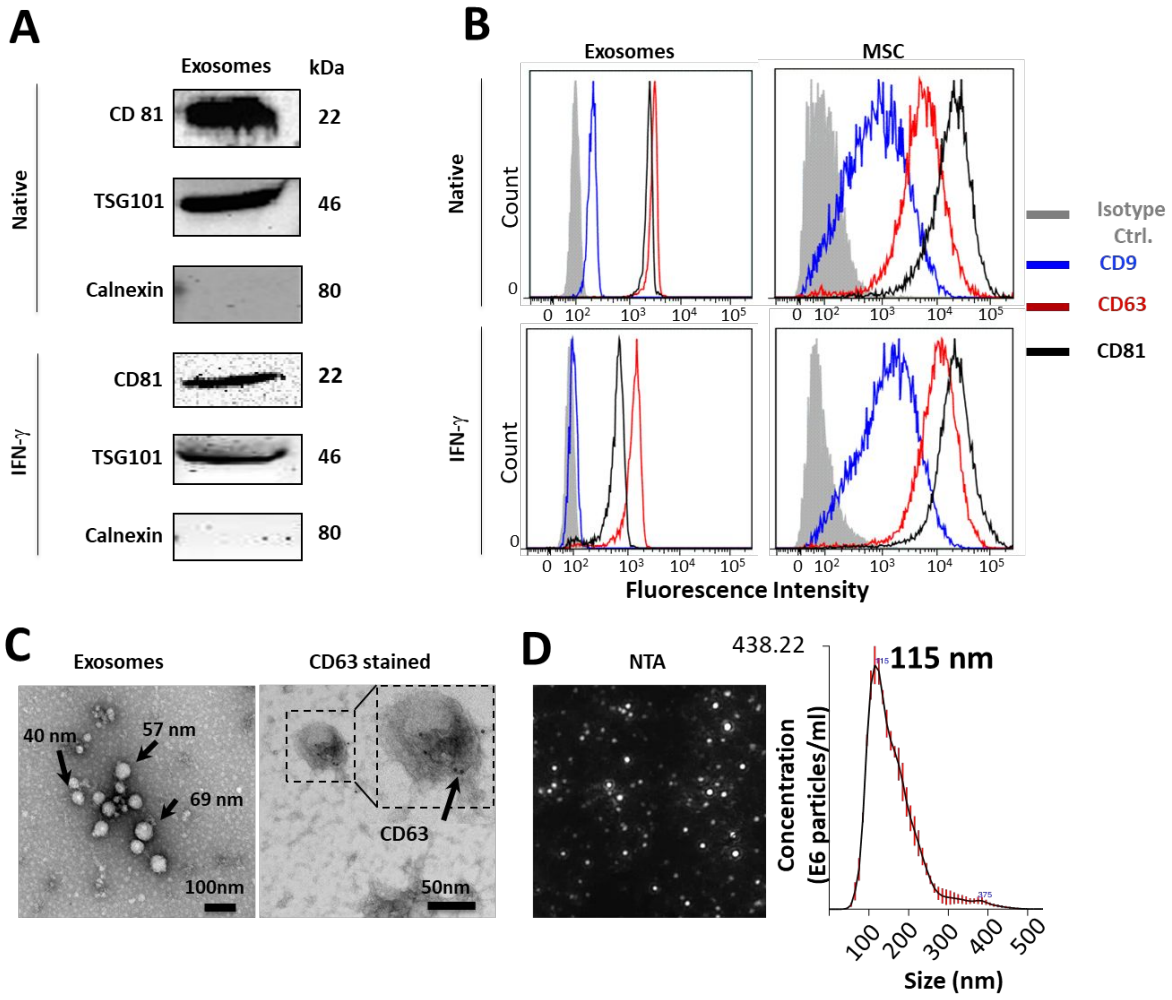

Figure S2. Characterization of MSC-derived exosomes. A) Western blotting of MSC-derived exosomes for CD81, TSG101 and Calnexin. B) Flow cytometry analysis of CD9, CD63 and CD81 expression on MSC exosomes bound to anti-CD63-coated beads and MSC. C) Electron microscopy images of native MSC exosomes (left) and exosomes using immunogold staining against CD63 (right). D) Representative captured screen shot of video of particles scattering light with the dilution (1/100) of the IFNγ-Exo as prepared (left); Representation of particle size (nm) and concentration (particles/ml) (right) analyzed using nanoparticle-tracking analysis (NTA).

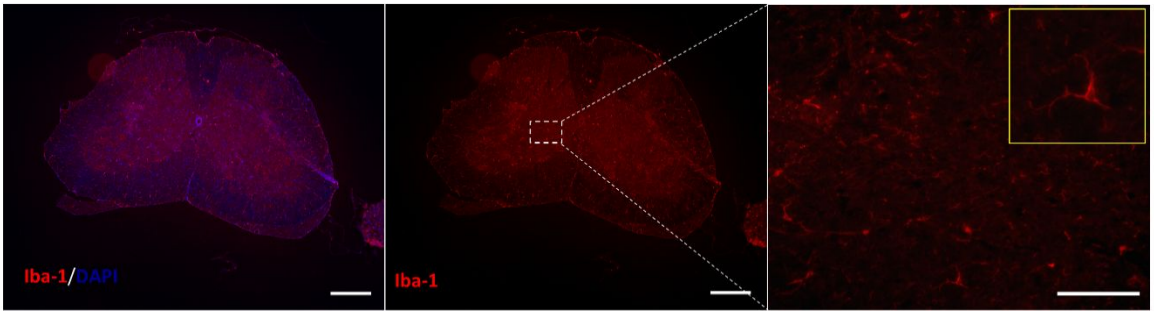

Figure S3. Immunohistochemistry of Iba-1, indicative of resident resting macrophages/microglia, and the nuclear stain DAPI in control healthy group. Yellow inset frames are magnified images showing the morphology of macrophages. Left and middle panel Scale: 400 μm; Right panel Scale: 80 μm.

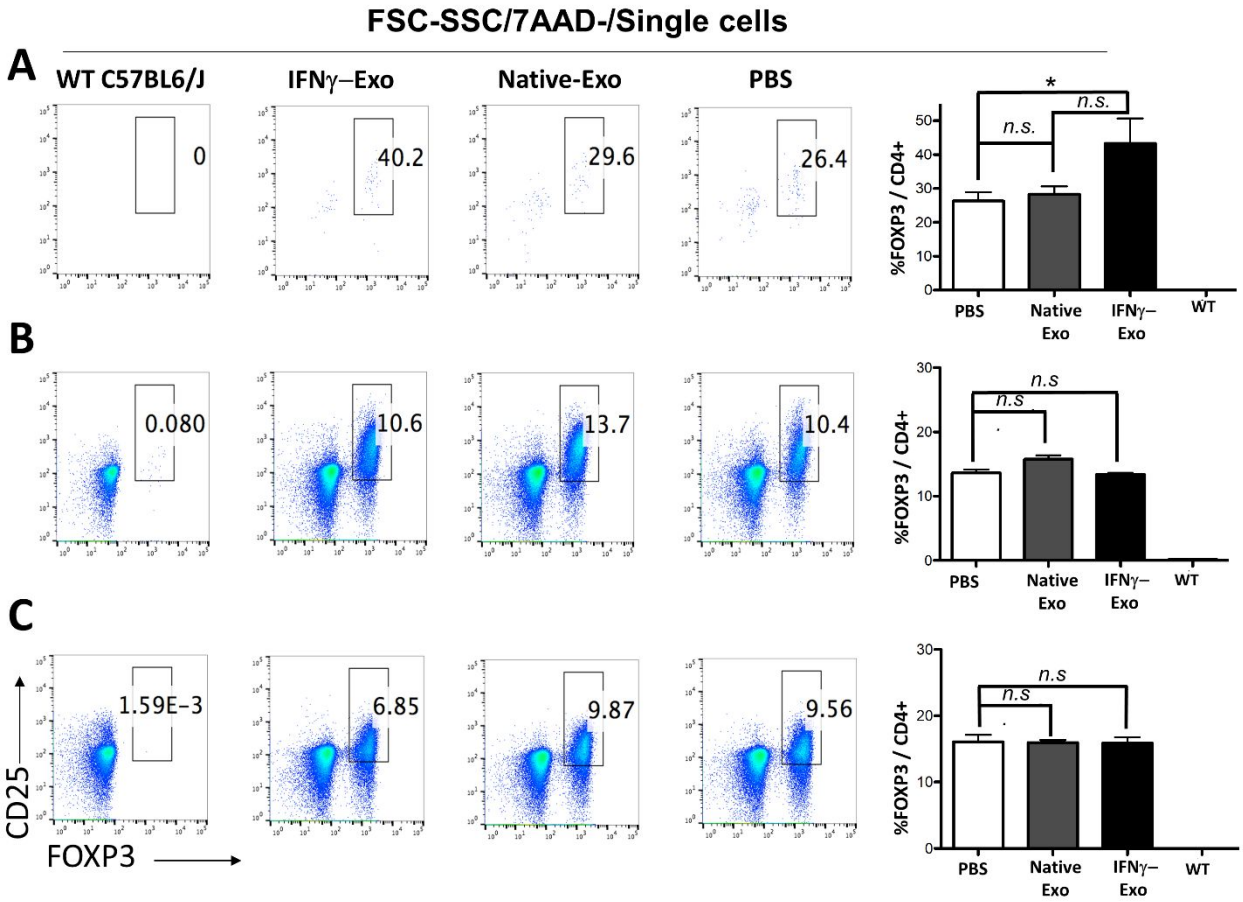

Figure S4. Representative flow cytometry plots and their quantification of CD4+CD25+FOXP3+ Tregs within A) spinal cords B) spleens and C) lymph nodes of PBS (n=3) of Native Exo (n=3), and IFNγ-Exo (n=3) treated EAE mice. Unpaired t-tests were used to determine *p* values. (*n.s.* non-significant, **p* < 0.05; ***p* < 0.01).

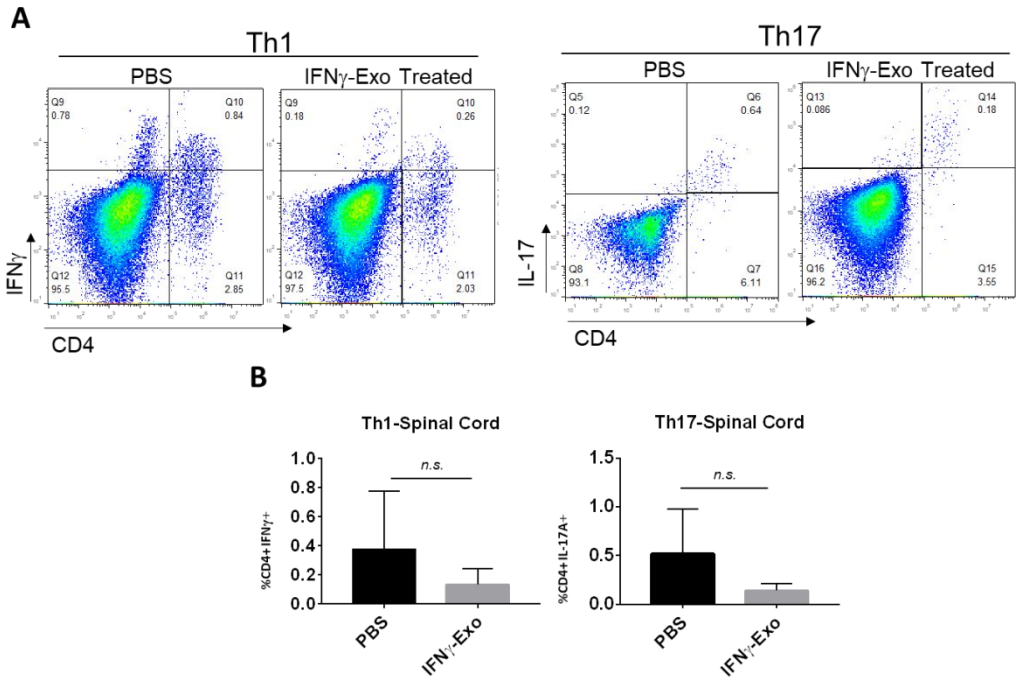

Figure S5. A) Representative flow cytometry plots and their quantification for spinal cords of PBS (n=3) and IFNγ-Exo (n=3) treated EAE mice, gated for CD4+IFNγ+ and CD4+IL-17A+ as representatives of Th1 and Th17, respectively. B) Plots are quantified for Th1/Th17. Unpaired t-tests were used to determine *p* values. (*n.s.* non-significant).

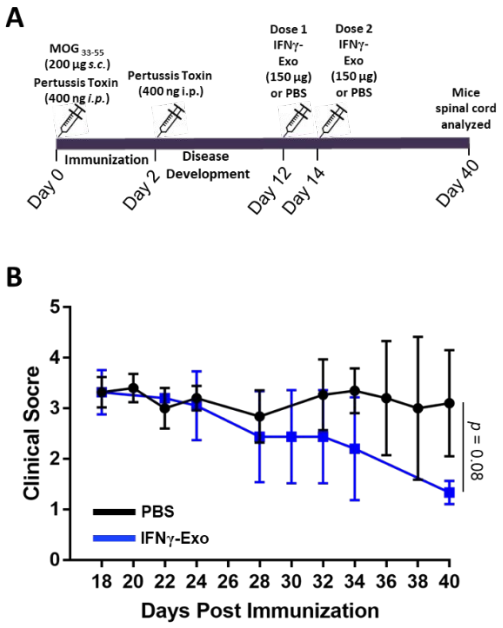

Figure S6. A) Schematic representation of early intervention procedure to treat EAE mice. IFNγ activated UC-MSC derived Exosomes (IFNγ-Exo) or PBS were injected *i.v.* to mice at days 12 and 14 (before disease peak, n=4 for each group). B) IFNγ-Exo treatment led to a robust trend toward decreased clinical score that neared significance (p=0.08). Clinical scoring was conducted from day 18 till day 40 after immunization. Mann-Whitney t-tests were used to determine the *p* values.

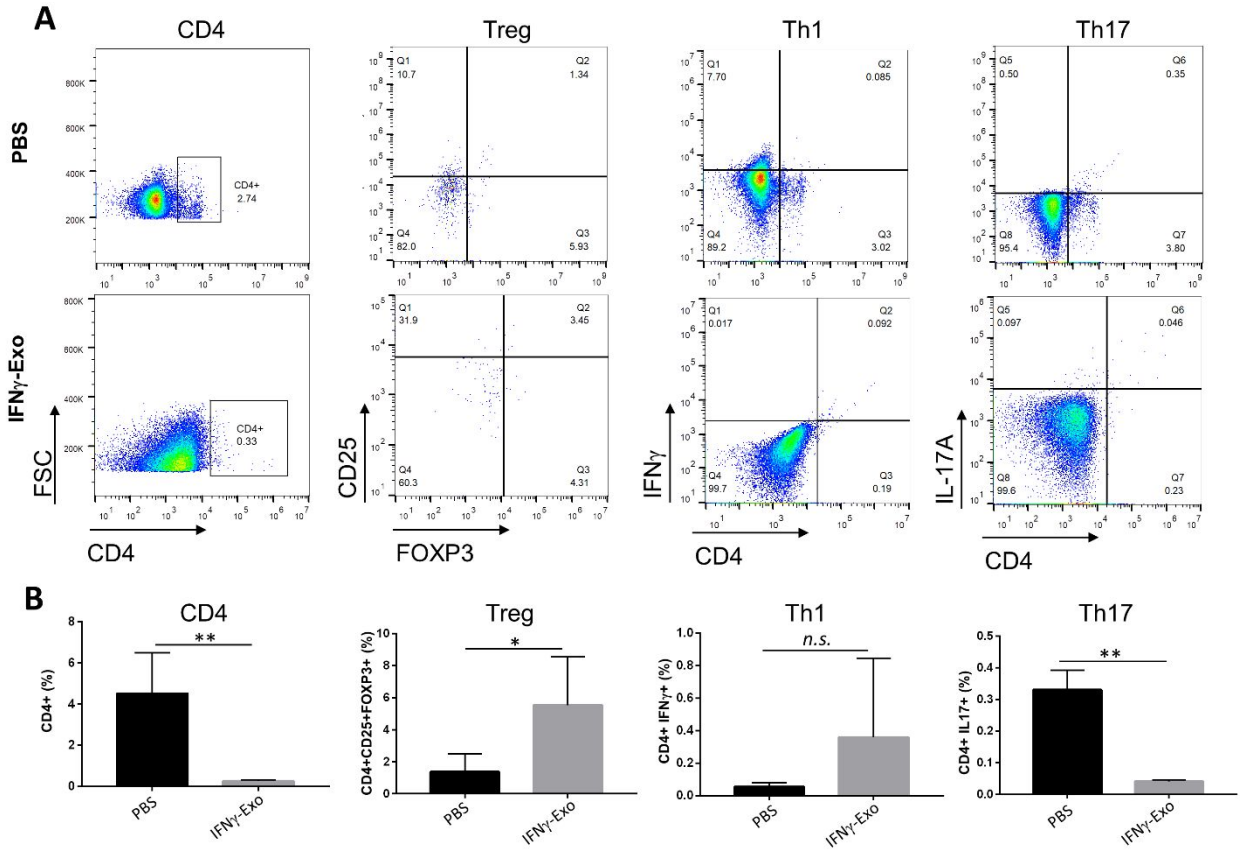

Figure S7. A**)** Representative flow cytometry plots and their quantification for spinal cords of PBS (n=3) and IFNγ activated UC-MSC derived Exosomes (IFNγ-Exo) (n=3) treated mice, gated for CD4, Th1, Th17, and Treg, and B) their corresponding quantifications. Unpaired t-tests were used to determine *p* values. (*n.s.* non-significant, **p* < 0.05; ***p* < 0.01).

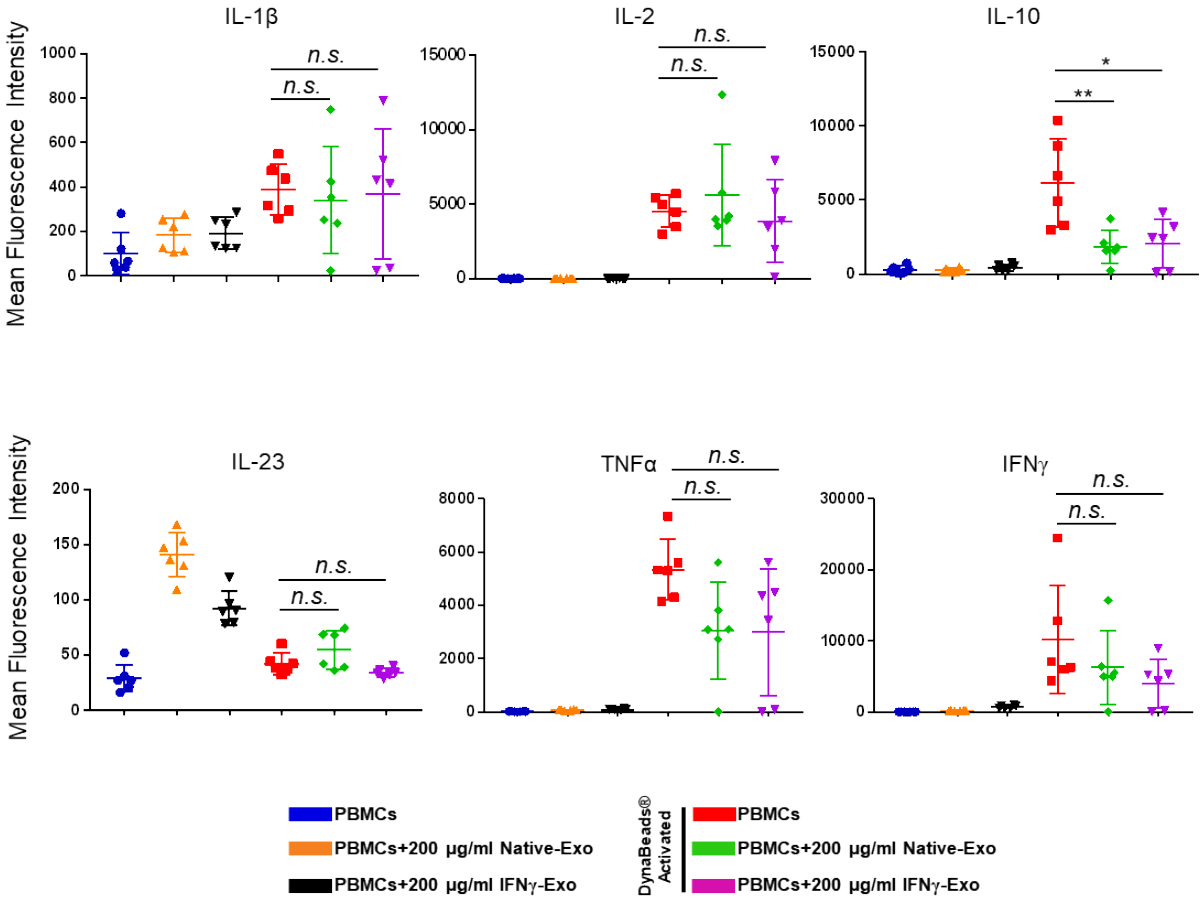

Figure S8. Human PBMCs stimulated for 4 d with Dyna® beads, in the absence or presence of exosomes produced by native or IFNγ-stimulated MSCs. Supernatants were harvested and secreted cytokine analyzed using Luminex MAGPIX™. Unpaired t-tests were used to determine *p* values. (*n.s.* non-significant, **p* < 0.05; ***p* < 0.01).

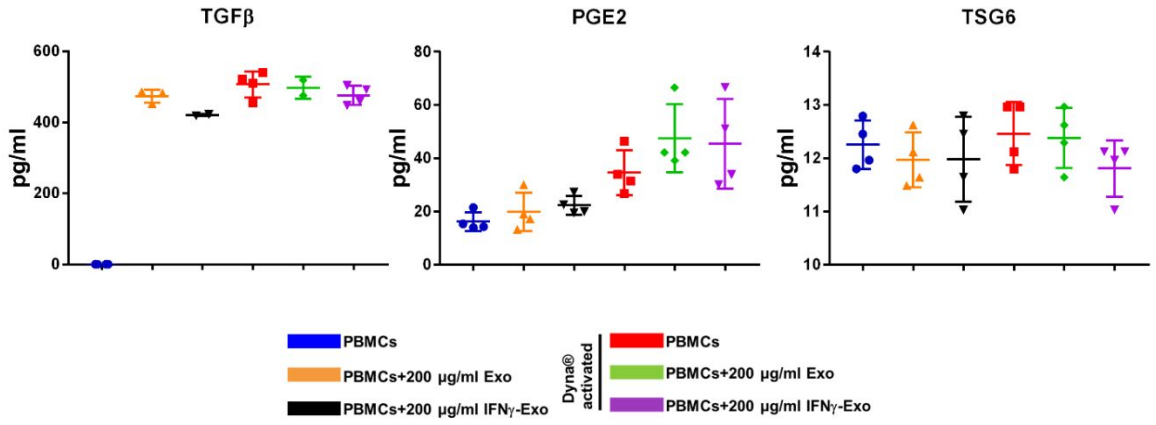

Figure S9. Human PBMCs were stimulated with DynaBeads® in the presence and absence of exosomes. Supernatants harvested and secreted cytokine analyzed using ELISA.

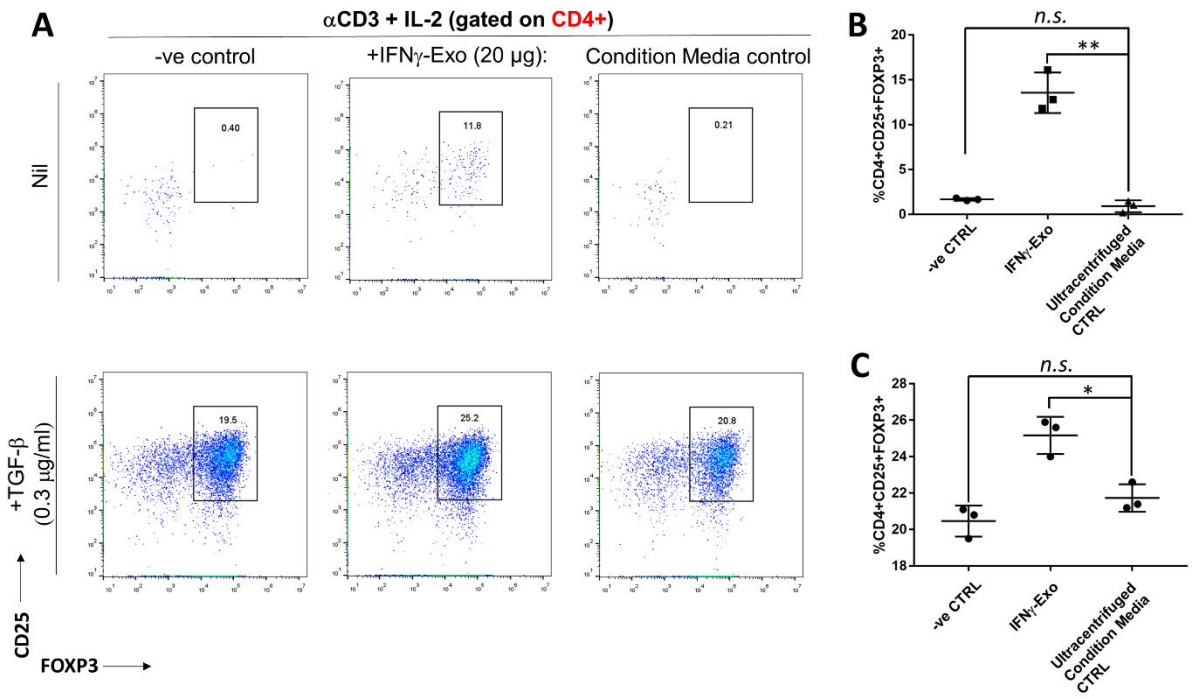

Figure S10. Ultracentrifuged culture media with EV depleted serum could not induce Treg in vitro. A) While IFNγ-Exo induce Tregs in the presence and absence of TGFβ, non-condition media control does not show significant Treg induction in the splenocyte in vitro culture. B) There was no statistical difference between number of CD4+CD25+FOXP3+ cells in the absence and C) presence of TGFβ compared to negative control. Unpaired t-tests were used to determine *p* values. (n=3 for each group; *n.s.* non-significant $*p < 0.05$; $**p < 0.01$).

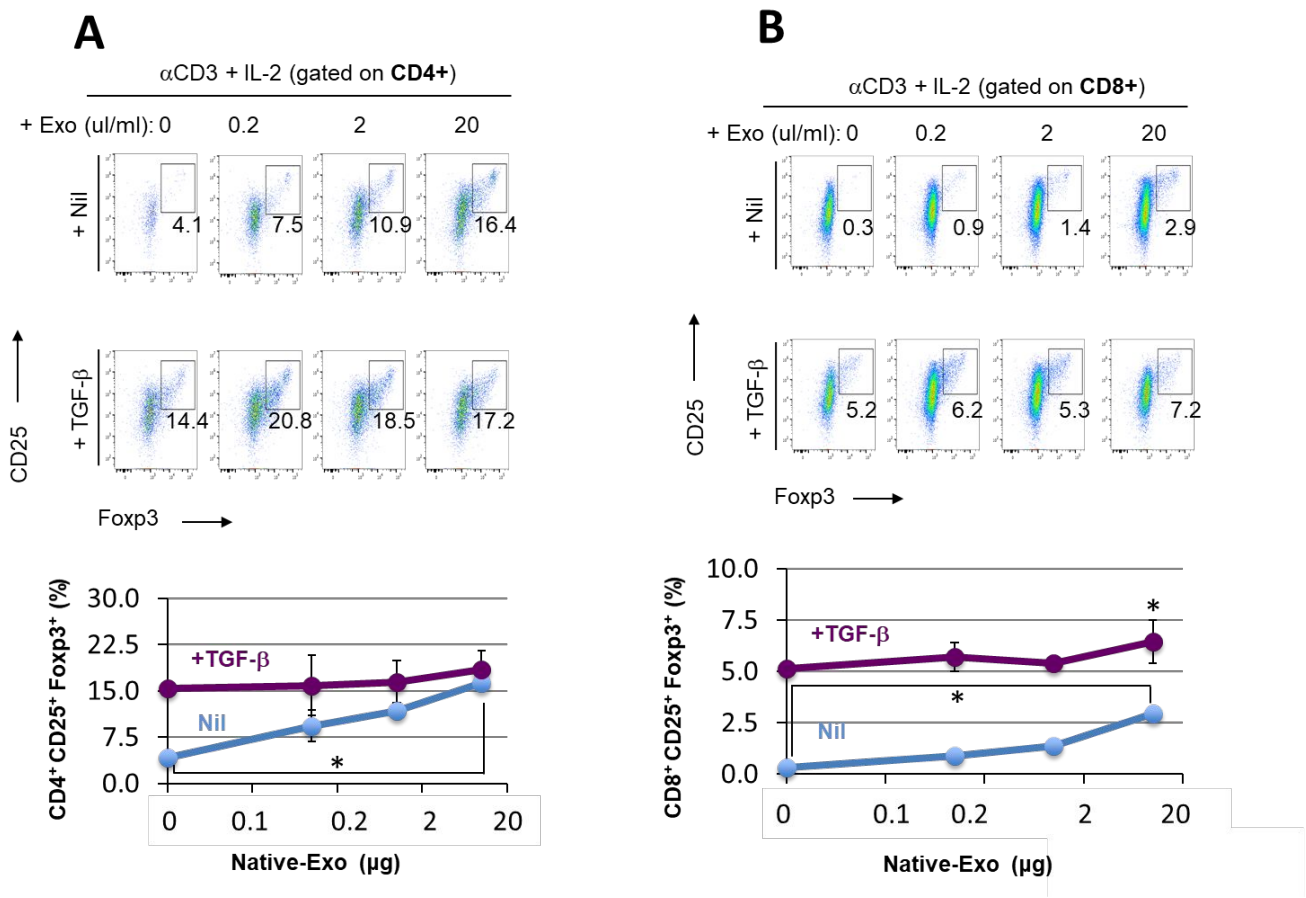

Figure S11. FOXP3-eGFP mice splenocytes were stimulated with anti-CD3 + IL-2 with or without TGFβ, and were further cultured in the presence of indicated concentrations of Native-Exo. Representative flow cytometry plots of CD4+ gate (A) or CD8+ gate (B). Statistical analyses were conducted between 0 µg and 20 µg Native-Exo (n=3 per concentration; *p < 0.05). Unpaired t-tests were used to determine p values.

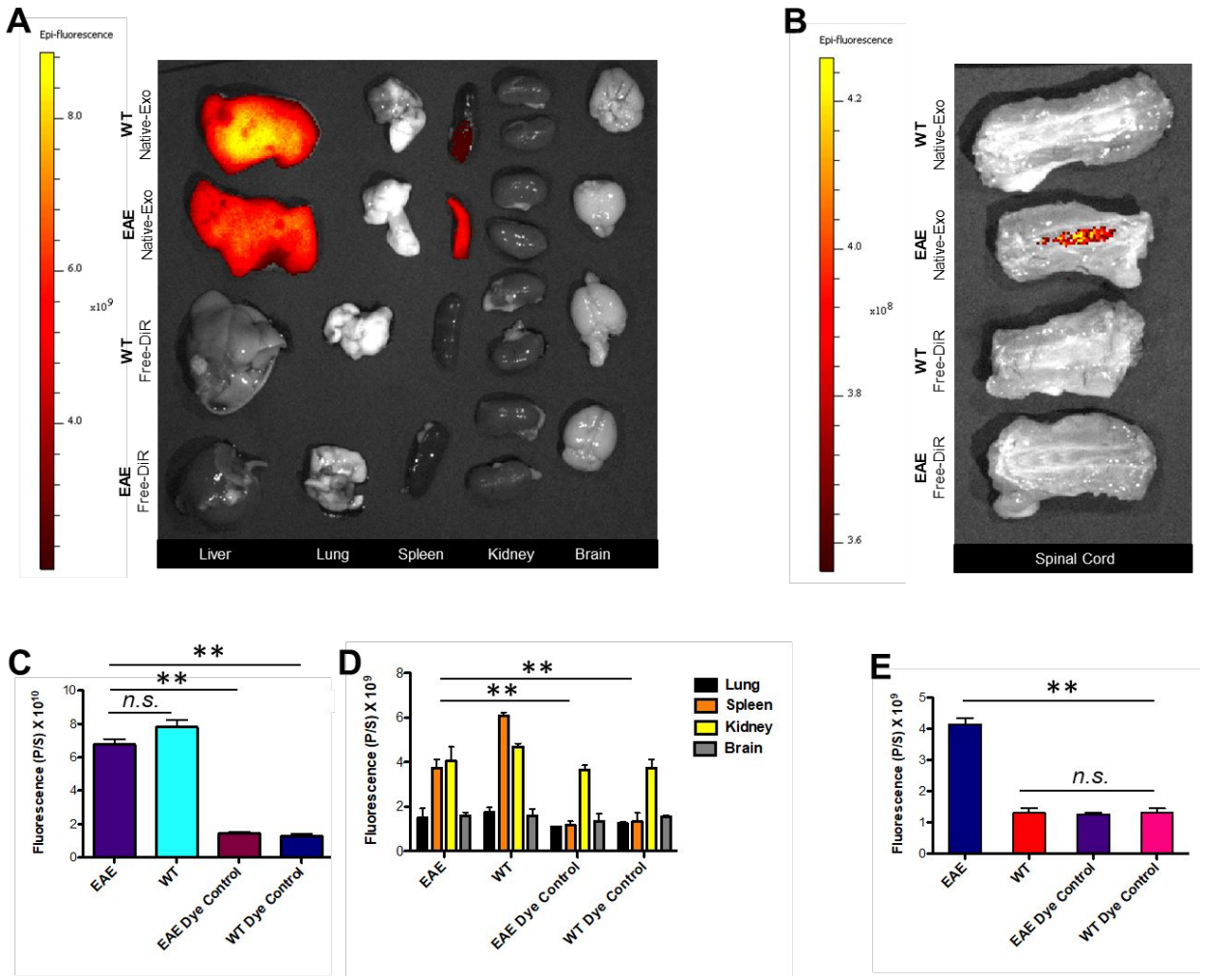

Figure S12. **Biodistribution of Native-Exo *in vivo*.** A) Representative IVIS images of different organs harvested at 3 hours following i.v. infusion of DiR labeled Native-Exo into healthy and EAE mice. Control groups received DiR dye alone (EAE-DiR, WT-DiR) to determine the background. B) Representative IVIS images of spinal cords 3 hours post injection of DiR labeled Native-Exo. C, D) Quantification of the fluorescent signal in different organs including liver, spleen, kidney, brain and lung at 3 hours following infusion of DiR labeled Native-Exo. (n=3; *n.s.* non-significant, $**p < 0.01$). E) Quantification of the fluorescent signal in spinal cords at 3 hours post injection of DiR labeled Native-Exo. (n=3; *n.s.* non-significant, $**p < 0.01$). Unpaired t-tests were used to determine *p* values.

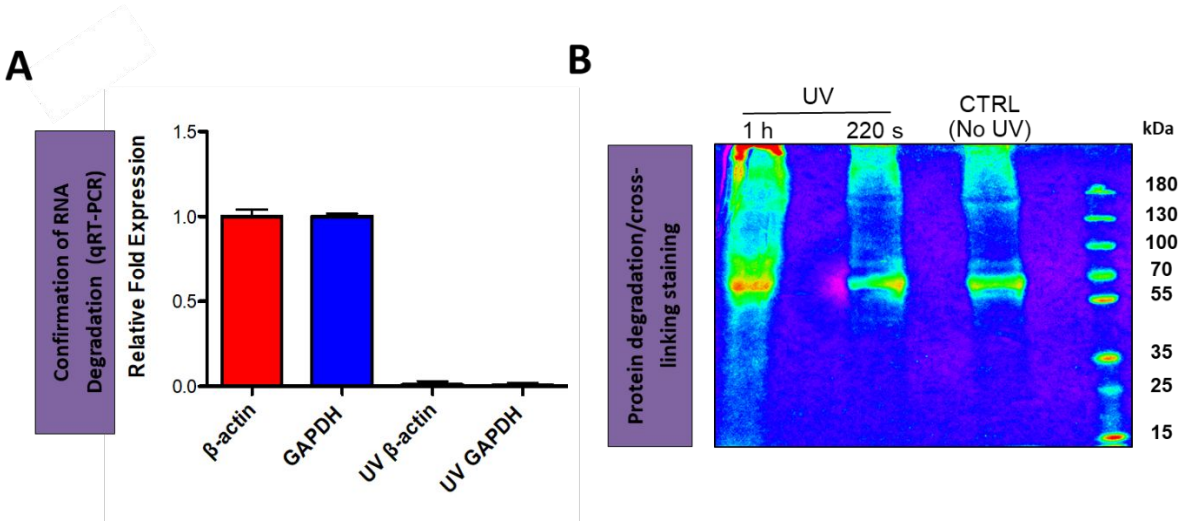

Figure S13. Inactivation of exosomal RNAs using UV. A) qRT PCR for β-actin (IFNγ-Exo) and GAPDH (Native-Exo) which confirms inactivation of RNA. 220 s UC exposure data was shown in this panel. B) Blue BANDit™ protein staining experiment showing exosomal protein crosslinking and degradation following 1 h UV treatment.

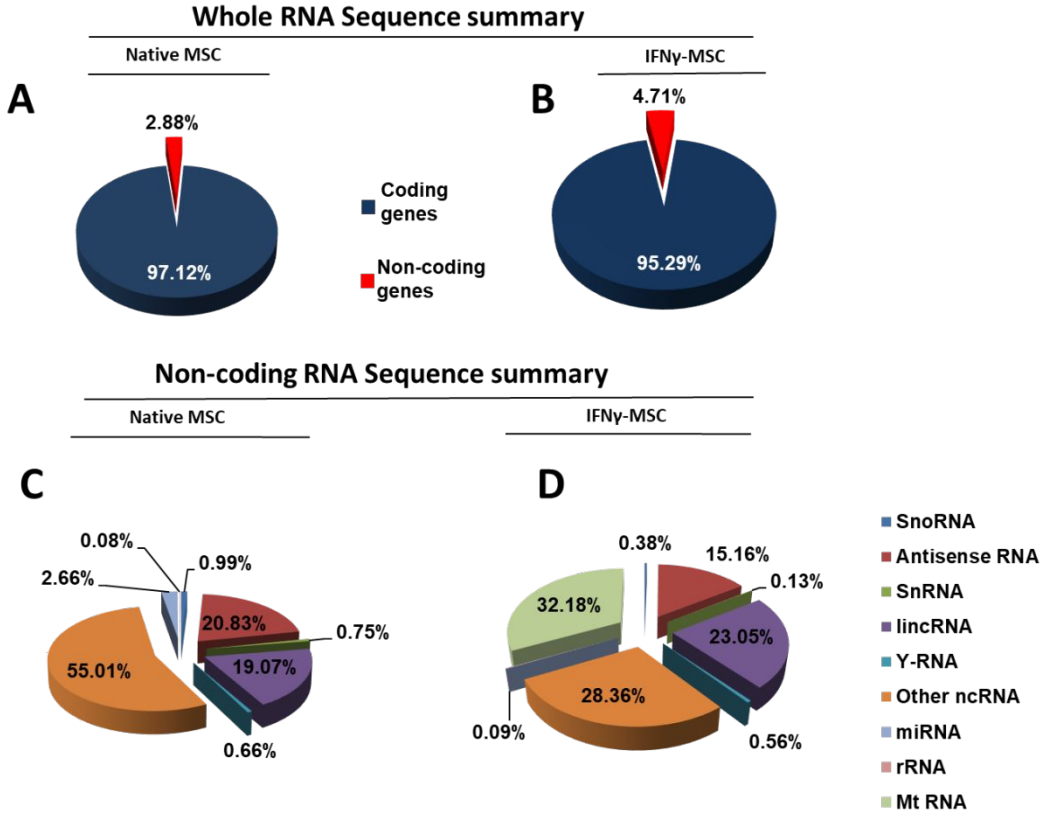

Figure S14. Deep RNA whole transcriptome analysis of native MSC and IFNγ-MSC. A) Whole RNA sequence summary of Native MSC. B) Whole RNA sequence summary of IFNγ MSC C) Non-coding RNA sequence summary (percentage of different types of non-coding RNAs) of Native MSC. D) Non-coding RNA sequence summary (percentage of different types of non-coding RNAs) of IFNγ MSC.

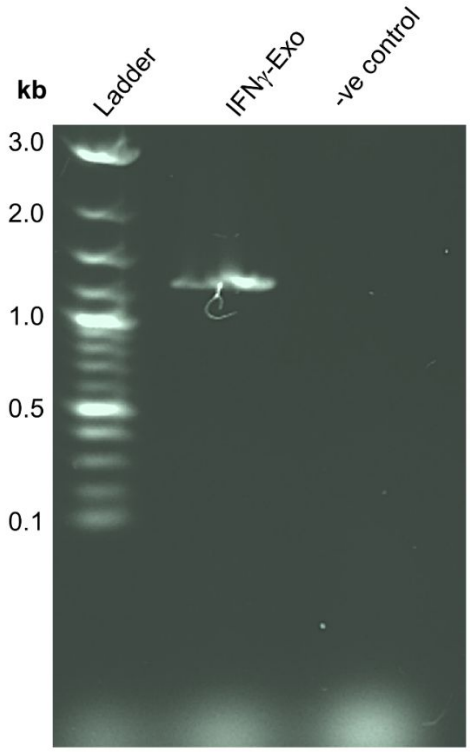

Figure S15. RT-PCR assay showed the presence of IDO1 mRNA within IFNγ-Exo. Resultant RT-PCR amplicons are approximately 1.2 kb, which is the size of full-length IDO-1 mRNA.

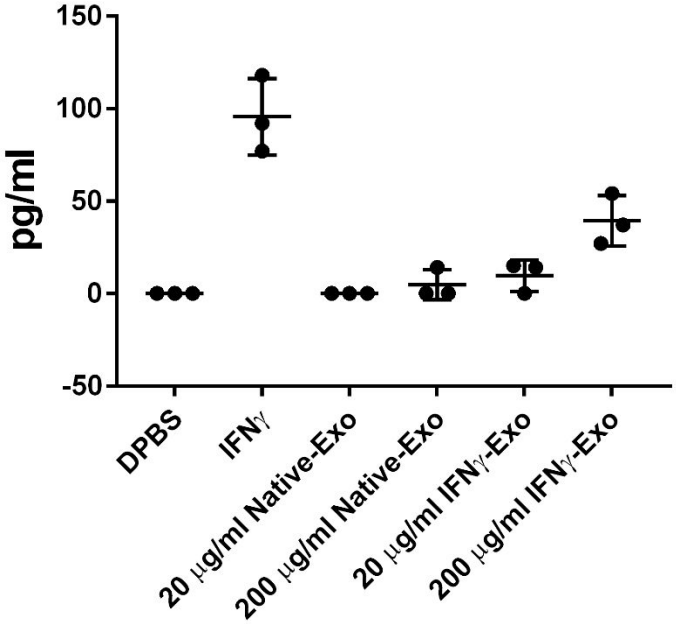

Figure S16. ELISA assay was conducted to measure the residual IFNγ from the culture medium to the IFNγ-Exo. 0.1 ng/ml of human IFNγ was used as a positive control.

Table S1. Most abundant RNA transcripts in the exosome fraction.

Gene Symbol	Gene Name	IFN-γ-Exo	Native-Exo
HSP90AA1	heat shock protein 90kDa alpha	621	575
SOD1	Superoxide dismutase 1	290	269
ACTB	actin, beta	13009	12091
S100A10	S100 calcium binding protein A10	1632	1746
ANXA1	annexin A1	467	493
TPM4	tropomyosin 4	4228	5263
MYL9	myosin, light chain 9, regulatory	2112	2613
GAPDH	glyceraldehyde-3-phosphate dehydrogenase	11494	12636
TMSB10	thymosin beta 10	8439	5482

Table S2. Pathway analysis miRNA in IFNγ-Exo using ingenuity database.

Top canonical pathways	Number of affected genes
Molecular Mechanisms of Cancer	34/365
Pancreatic Adenocarcinoma Signaling	19/106
PI3K/AKT Signaling	19/123